Targeting LOXL2 Improves Arterial Stiffness and Function in Angiotensin II-induced Hypertension in Males but not Females.

Huilei Wang[1*], Marta Martinez Yus[2*], Travis Brady[1], Rira Choi[3], Kavitha Nandakumar[3], Logan Smith[1], Rosie Jang[4], Bulouere Princess Wodu[5], Diego Almodiel[2], Laila Stoddart[1], Deok-Ho Kim[1,6,7,8], Jochen Steppan[2] and Lakshmi Santhanam[1,2,3,8,#]

[1]Department of Biomedical Engineering, Johns Hopkins University School of Medicine, Baltimore MD

[2] Department of Chemical and Biomolecular Engineering, Johns Hopkins University, Whiting School of Engineering, Baltimore, MD

[3] Department of Anesthesiology and CCM, Johns Hopkins University School of Medicine, Baltimore MD

[4] Department of Molecular & Cellular Biology, Johns Hopkins University, Krieger School of Arts and Sciences, Baltimore MD

[5] Department of Biology, Johns Hopkins University, Krieger School of Arts and Sciences, Baltimore MD.

[6]Division of Cardiology Department of Medicine, Johns Hopkins University School of Medicine, Baltimore MD

[7]Department of Mechanical Engineering, Johns Hopkins University, Whiting School of Engineering, Baltimore, MD

[8]Center for Microphysiological Systems, Johns Hopkins University, Baltimore, MD

[*]These authors contributed equally

[#]To whom correspondence should be addressed

720 Rutland Ave, Ross 1150

Baltimore MD 21205

USA

Email: Lsantha1@jhmi.edu

Abstract

Background: Hypertension accelerates arterial stiffening associated with natural aging. Aortic stiffness is both a cause and a consequence of isolated systolic hypertension. We identified lysyl oxidase-like 2 (LOXL2), a key matrix remodeling enzyme, as a potential therapeutic target for treating vascular stiffening. Here, we determine if LOXL2 depletion is protective against hypertension induced arterial stiffening, and we elucidate the sex differences present.

Methods: Angiotensin II (Ang II) pumps were implanted in *Loxl2*$^{+/-}$ and WT mice. Blood pressure and pulse wave velocity were measured noninvasively to assess hypertension and aortic stiffness. Wire myography and uniaxial tensile testing were used to test aortic vasoreactivity and elastic properties. Histological analysis and Western blotting determined vascular wall properties. The effect of biomechanical strain on LOXL2 expression and cell alignment was determined via uniaxial cell stretching.

Results: Ang II infusion induced hypertension in WT and *Loxl2*$^{+/-}$ mice, and arterial stiffening was ameliorated in *Loxl2*$^{+/-}$ male mice. LOXL2 depletion protected males from Ang II mediated potentiation of vasoconstriction, and attenuated passive arterial stiffening. Histological analysis showed increased aortic wall thickness and intralamellar distance with Ang II. Western blotting revealed an increase of LOXL2 accumulation and processing in hypertensive mice. Increased cyclic strain contributed to upregulation of LOXL2 in the aorta with induced hypertension.

Conclusions: Arterial stiffening is increased with Ang II infusion; however, it is ameliorated in *Loxl2*$^{+/-}$ male mice compared to WT despite developing Ang II-induced hypertension. This rise in arterial stiffness is driven by both VSMC response and matrix remodeling.

Introduction

Hypertension is one of the major risk factors for cardiovascular diseases, including coronary artery disease, cardiac hypertrophy, atrial fibrillation, stroke, heart failure, and renal failure[1-6]. The global prevalence of hypertension has been increasing in the past four decades, to an estimated 31.1% in the global adult population[7]. Though awareness and treatment of hypertension has improved, only 43.4% of US patients with documented hypertension are able to successfully manage high blood pressure[8]. One of the consequences of uncontrolled hypertension is the acceleration of arterial stiffening noted with natural aging[9]. Because aortic stiffening is both a cause and a consequence of hypertension[10], an insidious loop of stiffening occurs and this exacerbates cardiovascular deterioration. Therefore, it is of high clinical interest to target arterial stiffening in the context of hypertension.

LOXL2 is a member of the lysyl oxidase (LOX) family of amine oxidases, that catalyze collagen cross-linking, and therefore are essential enzymes for extracellular matrix (ECM) remodeling. Prior studies have identified LOXL2 as a potential therapeutic target in aging associated vascular stiffening[11] and shown higher levels of LOXL2 activity in aortic extracellular matrix in aged mice[11,12]. LOXL2 has also been shown to play a role in the development of various cardiovascular diseases including cardiac interstitial fibrosis, atrial fibrillation, and cerebral aneurysm[13-17]. In this study, we evaluated whether LOXL2 is activated by elevated biomechanical strain that occurs in hypertension and if LOXL2 depletion is protective against hypertension induced arterial stiffening.

Methods

Animal model: LOXL2 gene was disrupted by inserting a long terminal repeat (LTR)-trapping cassette in exon 1 as previously described[11]. *Loxl2*$^{+/-}$ mice were bred in-house and genotyped by PCR of tail biopsy. Male and female wild-type (WT) and *Loxl2*$^{+/-}$ littermates were used in this study. Additional age-matched C57BL/6J mice were purchased from the Jackson Laboratory to supplement the male and female WT groups. All procedures involving animals were approved by the Institutional Animal Care and Use Committee of the Johns Hopkins University. Mice were maintained in the Johns Hopkins University School of Medicine animal care facility, fed and watered ad libitum in a temperature-controlled room with a 12:12-hour light/dark cycle.

Blood pressure (BP) measurement: BP was measured non-invasively in conscious mice using the CODA noninvasive tail-cuff BP system (Kent Scientific Corporation). Mice were first gradually acclimated to being restrained in the mouse holders over 10 days. Mice were maintained at 37° C during measurement. BP was measured at baseline (immediately preceding Ang II pump placement), and then weekly after initiation of Ang II infusion. At least 5 measurements were recorded for each mouse for each time point, and then averaged.

Pulse-wave velocity (PWV) measurement: PWV, the gold-standard index of in vivo arterial stiffness, was measured noninvasively using high-frequency Doppler (Indus Instruments) as previously described[18]. Briefly, mice were placed supine on a heated (37°C) pad under anesthesia with 1.5% isoflurane. Pulsed Doppler signals and ECG were simultaneously captured at a thoracic and an abdominal aortic site. PWV (m/s) was calculated as the distance between these two locations, divided by the pulse transit time calculated using the foot-to-foot method.

Hypertension model: Hypertension was induced by Angiotensin II infusion (Ang II; 1000 ng/kg/min) via osmotic mini pumps (Durect Corp) in male and female WT and *Loxl2*$^{+/-}$ mice (**Fig 1A**, n = 11-12 per cohort) as follows: After baseline BP and PWV measurement, 12-14 weeks old WT and *Loxl2*$^{+/-}$ mice were randomized into hypertension and control groups. For pump implantation, mice were anesthetized with 1.5% isoflurane and underwent subcutaneous implantation of osmotic minipumps filled with Ang II solution in PBS (Sigma-Aldrich). For analgesia, mice received acetaminophen-treated drinking water (1.6 – 3.2 mg/ml) for 24 hours prior surgical procedure and for 2 days after the procedure. Controls underwent sham surgery. BP and PWV were measured weekly after surgery for 3 weeks. At the end of the study period (3 weeks of Ang II infusion), body weight was measured, and the aorta and heart were dissected out. The aorta was cleaned, cut into 2-mm rings, and used immediately for tensile testing and wire myography, fixed in 4% formaldehyde for histology, and flash-frozen for Western blotting.

Wire myography: Vasoreactivity of the aortic rings was examined as previously described[11,19]. Briefly, freshly dissected aortic rings (2 from each mouse) were mounted in the chamber of a wire myograph (DMT) in oxygenated Krebs-Ringer bicarbonate solution (in mM: 118.3 NaCl, 4.7 KCl, 1.6 CaCl2, 1.2 KH2PO4, 25.0 NaHCO3, 1.2 MgSO4, and 11.1 dextrose) at 37°C and pre-stretched to 600 mg-force. Maximal

contractility elicited by potassium chloride (KCl) was measured. After washing, vasocontractile response to increasing concentrations of phenylephrine (PE; 10^{-9}–10^{-5} mol/L) was measured. Next, endothelium-dependent (acetylcholine; ACh; 10^{-9}–10^{-5} mol/L) and endothelium-independent (sodium nitroprusside; SNP, 10^{-9}–10^{-5} mol/L) vasorelaxation of vessels preconstricted with PE (10^{-6} mol/L) was determined. All reagents used in wire myography were purchased from Sigma Aldrich.

Tensile Testing: The mechanical properties of the intact and decellularized aortic rings were determined by uniaxial tensile testing as previously described[20-23]. Two intact and two decellularized aortic rings from each mouse were tested. Samples were decellularized following published protocols[20] with minor modifications. Briefly, aortic rings were placed in a decellularization solution of 1% SDS and 3.3% NH_4OH in H_2O, and gently rocked for 1 h at room temperature on an end-to-end shaker. Samples were then washed with 3.3% NH_4OH in H_2O (30 min, gentle rocking), followed by 3 washes (15 min each) in phosphate buffered saline (PBS, pH 7.4; ThermoFisher; containing antibiotic-antimycotic (1x, ThermoFisher)). Removal of cells was verified by the absence of DNA (Pico Green assay kit; Invitrogen), and the absence of GAPDH in the aorta homogenate by Western blotting.

For tensile testing, vessel lumen diameter (*Di*), wall thickness (*t*), and sample length (*L*) were first determined by microscopy for each sample. Samples were mounted on the pins of an electromechanical puller (DMT560; Danish Myo Technology A/S). After calibration and alignment, the pins were moved apart using an electromotor and displacement and force (*F*) were recorded continuously until sample failure. Engineering stress (*S*) was calculated by normalizing force (*F*) recorded with stress-free ring cross-section area ($S = F/2t \times L$). Engineering strain (λ) was calculated as the displacement divided by *Di*. The stress–strain relationship was represented by the equation $S = \alpha \exp(\beta\lambda)$ where α and β are constants. α and β were determined by nonlinear regression for each sample and used to generate stress-strain curves.

Cell Culture: Human aortic smooth muscle cells (HASMCs, ThermoFisher) were cultured in smooth muscle cell media (ScienCell) containing 2% fetal bovine serum, SMC-growth supplement, and antibiotic-antimycotic. LOXL2-depleted HASMC (T1) cells were generated by targeting the *Loxl2* gene by CRISPR-Cas9 gene editing as previously described[12]. Human Aortic Endothelial Cells (HAECs) were cultured using complete endothelial cell media (ECM; ScienCell) with 5% FBS, endothelial cell growth supplement antibiotic-antimycotic. All cells were cultured in humidified incubators with 5% CO_2 at 37°C. To obtain LOXL2 enriched media, LOXL2 was overexpressed by adenoviral transduction as previously described. Prior to use, cells were authenticated by immunofluorescent staining of α-SMA and SM22α for HASMCs and CD31 (PECAM) and VEGF-R2 for HAECs. For both cell types, 3 distinct lot numbers (representing 3 distinct donors; 50-55 year old Caucasian males with no reported co-morbidities (hypertension, type 2 diabetes, obesity)) were used.

Uniaxial cell stretching: To examine the effect of biomechanical strain on LOXL2 expression and cell alignment, HASMCs and HAECs were subjected to uniaxial cyclic mechanical stimulation using the Strex Cell Stretching System as follows: Cells were seeded on fibronectin coated PDMS chambers (150,000 cells/chamber for HASMCs,

and 680,000 cells/chamber for HAECs). Each chamber has 4cm^2 culture area. Cells were allowed to adhere and spread overnight and then serum starved for 24 h, and fresh media was provided to the cells. For HASMCs, three conditions were examined: 1) HASMC controls, 2) T1 (LOXL2 depleted), and 3) T1+ LOXL2, in which LOXL2-enriched media, prepared by adenoviral overexpression of LOXL2 in T1 cells was used. Samples were used for Western blotting or cell alignment analysis.

Cell alignment analysis: PDMS membranes subjected to stretch (0, 10, 20%) were fixed in 4% formaldehyde and stained with Alexa Fluor 488 Phalloidin (ThermoFisher) to visualize actin. Images were captured with a confocal microscope (Leica SP8) at 5x magnification and imported into CurveAlign V4 software (https://github.com/uw-loci/curvelets/) run on MATLAB (2021 edition, The MathWorks, Natick, MA) to determine fiber orientation using a fast discrete curvelet transform-based algorithm. The curvelet orientations and the associated alignment coefficient, kurtosis, standard deviation, and variance parameters were obtained using a boundary-free CT fiber analysis method and a 0.06 fraction of kept coefficients. Intensity of fibers in the same orientation is characterized by the alignment coefficient which ranges from 0 to 1 with 1 signifying completely aligned fibers. Cumulative compass plots of curvelet orientation for each condition were generated using a custom MATLAB script. Plots were normalized to the number of replicates and plotted with a bin size of 5 degrees.

Western blotting: Tissue specimens were homogenized, and cells were lysed in mammalian protein extraction reagent (M-PER; Thermo Fisher) containing protease inhibitors cocktail (Roche). Soluble proteins and insoluble matrix were separated by centrifugation at 10,000 x *g* for 15 minutes. A Bio-Rad protein assay was used to determine protein concentration in the soluble fraction. The insoluble matrix samples were resuspended in in 1.5x Laemmli buffer with DTT (New England Biolabs) in a normalized volume based on cytosolic protein concentration (50 µl per mg of soluble protein). Western blotting of tissue samples was performed using 25 µg of the soluble fraction, and 25 µl of the insoluble matrix. Secreted protein in cell culture media was enriched using StrataClean Resin (Agilent, 10 µl per 5 ml of media) as previously described[11,24].

Protein samples were resolved by SDS-PAGE and electro-transferred onto nitrocellulose membrane. Blots were stained with Ponceau S, imaged (BioRad ChemiDoc) and then blocked in 3% nonfat milk in TBST (Tris-buffered saline, 0.1% Tween 20). Blots were then incubated with primary antibody (1:1000, 2 h) washed and incubated with secondary antibody (1:10,000, 2 h). After 3 TBS-T washes, blots were developed with the Clarity Western ECL system (Bio-Rad). The following primary antibodies were used: LOX rabbit polyclonal (ThermoFisher PA1-46020), LOXL2 rabbit monoclonal (Abcam ab179810), Collagen Type I Polyclonal Antibody (Thermo Scientific 14695-1-AP), COLIV rabbit polyclonal (Assay Biotech C0157), beta Actin Loading Control Monoclonal Antibody (Invitrogen, MA5-15739), GAPDH mouse monoclonal (Novus Bio NB300221). Primary antibodies were validated using knockdown/knockout (LOX, LOXL2), using recombinant protein (Collagens), or through prior reports in the literature (actin, GAPDH). Secondary antibodies used were goat anti-mouse IgG (H+L)-HRP conjugate (Biorad 1706516), AffiniPure goat anti-rabbit IgG (H+L)-HRP conjugate (Jackson ImmunoResearch 111035144).

Histology: Fixed aortic samples were paraffin embedded and sectioned at 6 µm thickness with visible lumen and mounted onto charged slides (Reference Pathology Lab, JHU). Hematoxylin and eosin, Masson's trichrome, and Movat pentachrome stains were performed using standard methods and imaged with a Laxco microscope at x4, x10, x20 and x40 magnification. Lumen diameter, aortic wall thickness, intralamellar distance, and VSMC nuclei in the medial layer were determined using ImageJ software.

Results

LOXL2 depletion delays onset of Ang II induced hypertension in male mice. Systolic, diastolic, and mean blood pressure (BP) were measured in conscious mice immediately before (baseline) and during Ang II infusion weekly for a period of 3 weeks. Baseline BP values were similar across all groups (**Figure 1B, C; Supplemental Figure S1**). Systolic BP increased rapidly in WT males with Ang II infusion, with a statistically significant increase within 1 week, and remained elevated for the duration of the study period. In the *Loxl2*$^{+/-}$ males with Ang II treatment, the onset of hypertension was delayed compared to WT (**Figure 1B; Supplemental Figure S1**). In female mice with Ang II infusion, BP elevation was slower than in male counterparts, and a steady increase was observed in both WT and *Loxl2*$^{+/-}$ groups with Ang II infusion over the course of 3 weeks **(Figure 1C, Supplemental Figure S1).**

We also evaluated the effect of Ang II induced hypertension on body weight and heart weight/body weight as an index of cardiac hypertrophy. Consistent with prior studies[25-27], Ang II infusion resulted in a significantly lower body weight in WT males (vs. control WT males) **(Figure 1Di)**. *Loxl2*$^{+/-}$ control males had significantly lower body weight compared to WT controls and Ang II infusion did not result in lower body weight in *Loxl2*$^{+/-}$ males (vs. control *Loxl2*$^{+/-}$ males) (**Figure 1Di**). Cardiac hypertrophy (greater heart weight to body weight ratio) was observed with Ang II infusion in both WT and *Loxl2*$^{+/-}$ males when compared to normotensive counterparts (**Figure 1Dii**). In females, body weight was similar in all groups **(Figure 1Ei)**. Cardiac hypertrophy was noted in *Loxl2*$^{+/-}$ females with Ang II induced hypertension, while WT females exhibited a trend towards increased cardiac hypertrophy (**Figure 1Eii**).

LOXL2 depletion prevents elevation in PWV caused by Ang II-induced hypertension in males. PWV, the gold-standard index of in vivo aortic stiffness, was measured noninvasively at baseline and weekly during the 3-week period of Ang II infusion. PWV increased steadily in male WT mice over 3 weeks of Ang II infusion (**Figure 2A)** and increase in BP **(Figure 1B)** preceded the onset of significant PWV increase. In *Loxl2*$^{+/-}$ males, PWV was not significantly elevated **(Figure 2A)** despite the eventual development of hypertension with Ang II infusion (**Figure 1B**). In female mice, Ang II infusion did not lead to elevated PWV in either WT or *Loxl2*$^{+/-}$ groups (**Figure 2B**) despite the increase in systolic BP (**Figure 1C**). Heart rate was similar in all groups during PWV measurements (**Supplemental Figure S2**).

LOXL2 depletion protects males from Ang II mediated potentiation of vasoconstriction: Ang II induced hypertension is known to dysregulate vascular reactivity. Therefore, we next examined the changes in vascular reactivity responses by wire myography. Maximal vasoconstriction response to phenylephrine was observed in Ang II-treated WT males, but not in *Loxl2*$^{+/-}$ males (**Figure 3Ai**). EC50s were similar in all groups of male mice **(Figure 3Ai)**. Acetylcholine-induced endothelial-dependent vasorelaxation was significantly impaired with Ang II-induced hypertension in WT males and LOXL2 depletion was only partially protective (**Figure 3Aii**). Endothelial independent responses to sodium nitroprusside were independent of Ang II in males of both genotypes (**Figure 3Aiii**). In females, maximal contractility to phenylephrine was elevated with Ang II infusion in WT mice and to a larger magnitude in *Loxl2*$^{+/-}$ mice

compared to corresponding controls (**Figure 3Bi**). Endothelial dependent relaxation in response to increasing concentrations of acetylcholine was impacted by Ang II in WT mice only (**Figure 3Bii)**. Endothelial independent vasorelaxation elicited by sodium nitroprusside was similar in all groups **(Figure 3Biii)**.

LOXL2 depletion attenuates passive arterial stiffening: The passive stiffness of intact (native) and decellularized aorta was examined by tensile testing (**Figure 4)**. Ang II infusion resulted in a marked increase in passive stiffness of intact aortic rings from WT males **(Figure 4Ai)** but not in *Loxl2*$^{+/-}$ males **(Figure 4Aii)**. The incremental modulus at strains of 0.5 (elastin deformation) and 2.5 (collagen deformation) was also markedly elevated in intact rings from WT males **(Figure 4Aiii, iv).** Decellularized aortic rings from male WT mice that received Ang II were also stiffer than untreated counterparts (**Figure 4Bi**) but those from *Loxl2*$^{+/-}$ males did not exhibit increased stiffness with Ang II infusion (**Figure 4Bii**). The incremental modulus of decellularized aortae from WT males was significantly higher only at strain of 2.5 (**Figure 4Biii, iv**), suggesting that collagen accumulation is a key component of aortic ECM stiffening. Interestingly, Ang II induced hypertension resulted in elevated ultimate tensile strength (stress at failure) in the *Loxl2*$^{+/-}$ males in both the intact and decellularized aorta (**Figure 4Ci, ii**). Strain at failure was similar in the intact rings from males but was increased with Ang II infusion in decellularized rings from both WT and *Loxl2*$^{+/-}$ males **(Figure 4Di, ii).**

Intact aortae of both WT and *Loxl2*$^{+/-}$ females were protected from stiffening and exhibited no change in incremental elastic modulus at low (0.5) and high (2.5) strain **(Figure 4Ei, ii, iii, iv)**. Similarly, decellularized aortae of females did not show any change in material properties with Ang II infusion **(Figure 4Fi, ii, iii, iv)**. In females, stress at failure of intact rings remained unchanged in both genotypes with Ang II infusion (**Figure 4Gi**). However, decellularized rings of *Loxl2*$^{+/-}$ females that received Ang II showed higher ultimate stress when compared to both *Loxl2*$^{+/-}$ controls and WT females with Ang II infusion (**Figure 4Gii**). Strain at failure was higher in the *Loxl2*$^{+/-}$ females vs. WT littermate females and was unaffected by Ang II (**Figure 4Hi**). Decellularized segments from *Loxl2*$^{+/-}$ females exhibited higher strain at failure than both the WT females with Ang II as well as *Loxl2*$^{+/-}$ female controls (**Figure 4Hii**).

Together, these findings show that the vascular matrix is remodeled with Ang II infusion in WT males, contributing to vascular stiffening; this remodeling was largely ameliorated in *Loxl2*$^{+/-}$ males. Surprisingly, better material strength (maximal stress bearing capacity) is noted in the *Loxl2*$^{+/-}$ males and females with Ang II infusion compared to their normotensive counterparts.

Ang II-induced hypertension leads to aortic wall remodeling. We next examined whether aortic remodeling was LOXL2 dependent using Hematoxylin Eosin (H&E), Masson's trichrome, and Movat's pentachrome staining **(Figure 5Ai, Aii)**. Ang II infusion resulted in VSMC hyperplasia in WT males, reflected by the VSMC nuclei density in the vascular wall, but not in the *Loxl2*$^{+/-}$ males (**Figure 5Bi).** Ang II infusion did not impact VSMC numbers in the vascular wall of female mice (**Figure 5Bii**). Aortic lumen diameter was similar amongst all groups in both males and females (**Figure 5Ci, Cii**). Wall thickness increased with Ang II infusion in both WT and *Loxl2*$^{+/-}$ males but not females **(Figure 5Di, Dii).** Intralamellar distance was higher in both WT and *Loxl2*$^{+/-}$

males with Ang II infusion when compared to normotensive counterparts (**Figure 5Ei**). In females, intralamellar distance increased with Ang II infusion only in the *Loxl2*$^{+/-}$ group, and at baseline, WT females exhibited higher intralamellar distance than the *Loxl2*$^{+/-}$ littermates (**Figure 5Eii**).

LOXL2 accumulation and processing are increased in hypertensives. ECM crosslinking with an accumulation of collagens is a mechanism by which Lysyl oxidases (LOXs) can mediate arterial remodeling in Ang II induced hypertension. A qualitative increase in collagen content was noted with Ang II infusion by Masson's trichrome and MOVAT pentachrome staining in both WT and *Loxl2*$^{+/-}$ male mice and WT female mice **(Figure 5Ai, Aii).** However, the stains do not allow us to distinguish the specific subtypes of collagen, particularly Collagen I and IV, that are known substrates of LOXL2[24]. We therefore next evaluated LOX, LOXL2, Collagen I, and Collagen IV protein abundance in the aortic ECM by Western blotting. LOX is secreted as a pro-protein (~50 kDa) and requires processing by BMPs to release the active form (~25 kDa)[28]. While LOXL2 is active in its full-length form (~100 kDa), processing shifts its substrate preference from Collagen IV for the full-length form to Collagen I for the processed form (~65 kDa)[24]. Western blotting revealed elevated full length and processed LOXL2 in WT males with Ang II infusion (**Figure 6Ai-iii**). In the *Loxl2*$^{+/-}$ mice, although a strong trend towards increased levels of both full length and processed LOXL2 were noted with Ang II infusion, the data did not reach statistical significance (**Figure 6Ai-iii**). In males, pro-LOX and active LOX were similar in all groups although a trend towards increased active LOX was noted in the Ang II treated WT and *Loxl2*$^{+/-}$ groups (**Figure 6Ai, iv, v**). In males, Collagen I increased and Collagen IV decreased in the aortic ECM with Ang II treatment (**Figure 6Ai, vi, vii**). In females, full length and processed LOXL2 significantly increased with Ang II treatment in WT females but not in *Loxl2*$^{+/-}$ females although a strong trend was noted (**Figure 6Bi-iii).** Pro-LOX was similar in all groups, and active LOX was elevated only the *Loxl2*$^{+/-}$ females with Ang II infusion (**Figure 6Bi, iv, v).** Collagen I was markedly higher, and Collagen IV was lower with Ang II infusion in both WT and *Loxl2*$^{+/-}$ females (**Figure 6Bi, vi, vii)**.

When the sexes were grouped together to increase statistical power, we noted increased protein levels of full length and processed LOXL2 in both WT and *Loxl2*$^{+/-}$ mice with Ang II infusion versus untreated counterparts (**Supplemental Figure S3 A, B**). While full length LOX was similar in all groups, active LOX was elevated in the hypertensive WTs when compared with normotensive WTs, and a strong trend was noted in the *Loxl2*$^{+/-}$ hypertensives when compared with *Loxl2*$^{+/-}$ normotensive group **(Figure S3 C, D)**. Hypertension led to elevated ECM collagen I and reduced Collagen IV in both WT and *Loxl2*$^{+/-}$ mice **(Figure S3 E, F)**.

Cyclic strain upregulates LOXL2 expression in VSMCs but not ECs. To determine whether the overexpression of LOXL2 in the aorta with Ang II – induced hypertension is caused by biomechanical strain and to determine if ECs and SMCs both express and secrete LOXL2, we examined LOXL2 protein expression by human aortic smooth muscle cells (HASMC) and human aortic endothelial cells (HAEC) subjected to uniaxial stretching at 10% (normotensive) and 20% (hypertensive) stretch ratio[29,30]. Both HASMCs and HAECs aligned perpendicularly to the direction of stretch (**Figure 7Ai, Aii**). In HASMCs, 24 hours of 10% cyclic stretch did not alter LOXL2 abundance in the

secreted media or full length LOXL2 in the cell-derived ECM. However, abundance of processed LOXL2 was markedly elevated with increasing strain in the cell-derived ECM (**Figure 7Bi, ii**). In HAECs, LOXL2 level was highest at static state, and decreased significantly at both 10% and 20% stretch (**Figure 7Ci-iii),** suggesting that ECs are not a significant source of LOXL2 under normotensive or hypertensive strain. Thus, these results point to the VSMCs as the primary source of LOXL2 in the vascular media.

LOXL2 plays an important role in VSMC alignment. We next determined if LOXL2 facilitates VSMC alignment when exposed to stretch through catalytically dependent or catalytically independent mechanisms. To this end, we compared the alignment response of HASMCs in response to a hypertensive strain of 20% for 24 hours. Four groups were compared: 1) WT HASMC, 2) WT HASMC + PAT-1251, a specific inhibitor of LOXL2's catalytic function, 3) T1 HASMCs in which *Loxl2* gene was knocked-out by CRISPR-Cas9 gene editing, and 4) T1 HASMCs + AdLOXL2 (recovery of function) to reintroduce LOXL2 by adenoviral transduction. At the end of the uniaxial stretching period, LOXL2 abundance in the culture media determined by Western blotting (**Figure 8Ai**) confirmed loss of LOXL2 expression in the T1-HASMCs and recovery of LOXL2 expression in the T1-HASMCs+AdLOXL2. Samples were fixed, fluorescently labeled with FITC-Phalloidin, imaged by confocal microscopy, and analyzed with CurveAlign to determine the alignment coefficient (**Figure 8Aii, B)**. WT HASMCs oriented orthogonal to the stretch vector, as evidenced by the increase in alignment coefficient in 20% strain versus static (0%) condition. Both LOXL2 inhibition (PAT-1251) and knockout (T1 HASMC *Loxl2*$^{-/-}$ cells) diminished change in alignment coefficient with uniaxial strain. Importantly, Ad-LOXL2 restored the increase in alignment coefficient upon exposure to uniaxial strain in T1 cells. Together these findings suggest an important role for LOXL2 in mechanosensing and the involvement of its catalytic activity.

Discussion

In this study, we tested the effect of biological sex on Ang II-induced hypertension and whether central vascular stiffening in hypertension can be prevented by targeting LOXL2. The central findings are that development of hypertension and the associated stiffening of conduit vessels occurs through distinct mechanisms and timelines in males versus females during reproductive years when challenged with the same dose of Ang II. Specifically, males developed hypertension earlier with a larger magnitude of increase in BP than did females. While males also developed central arterial stiffening (indicated by higher PWV) following BP increase, females did not during the course of this study. Males lost body weight with Ang II infusion while females did not. In males, LOXL2 depletion delayed the onset of hypertension and was protective against development of in vivo arterial stiffening, indicated by PWV (**Figure 2**). In females with the slower but steady increase in BP, it is possible that later time points (>3 weeks) could lead to elevation in PWV, and this remains to be tested.

LOXL2 was previously shown to contribute to age-associated aortic stiffening via regulation of VSMC tone/reactivity and ECM remodeling. We therefore next examined vascular reactivity and passive aortic stiffness at the tissue level. Wire myography revealed sex-dependent vascular reactivity responses with Ang II induced hypertension.

We found that LOXL2 depletion prevented a hypercontractile response to phenylephrine in Ang II treated males, but not females. Male WT with Ang II infusion had impaired endothelial function, reflected in the attenuated relaxation response and higher EC50 with acetylcholine when compared with normotensive counterparts, and LOXL2 depletion prevented endothelial dysfunction in hypertensive males. Surprisingly, endothelial function was unimpaired in female WT hypertensives, while LOXL2 depletion resulted in reduced EC-dependent relaxation, independent of Ang II.

Tensile testing revealed that LOXL2 knockdown was protective against stiffening of the aortic ECM in males with Ang II induced hypertension, while WT exhibited marked stiffening. LOXL2 depletion also prevented VSMC hyperplasia in males. However, some evidence of remodeling was still noted in the aortae of *Loxl2*$^{+/-}$ males including an elevation in ultimate stress noted by tensile testing as well as increased wall thickness and intralamellar distance noted by IHC. Females again exhibited differences from males – Ang II infusion did not cause any change in passive stiffness in WT or *Loxl2*$^{+/-}$ females. The only evidence of remodeling was the increase in intralamellar distance as well as stress and strain at failure in Ang II treated female mice, and surprisingly, this was only in the *Loxl2*$^{+/-}$ females. Taken together, these findings show *Loxl2*$^{+/-}$ mice are still able to remodel the ECM. We therefore next tested if these changes arise from LOXL2 itself or whether there is a compensatory expression of prototypic LOX, typically shown to be activated in Ang II induced hypertension, in the *Loxl2*$^{+/-}$ mice.

At the molecular level, we found that Ang II infusion upregulated LOXL2 abundance in the aortic ECM and led to elevated levels of processed LOXL2 in both male and female WT mice. While the data did not reach significance in *Loxl2*$^{+/-}$ mice, a strong trend towards increased full length and processed LOXL2 was noted. Interestingly, in female *Loxl2*$^{+/-}$ mice, active LOX abundance was significantly higher with Ang II infusion, but not in *Loxl2*$^{+/-}$ males. Thus, females appear to have a compensatory increase in prototypic LOX activation following induction of experimental hypertension, but not males. Previous studies have shown that LOXL2 processing shifts its substrate preference from Collagen IV to Collagen I in VSMCs[24] and the prototypic active LOX also exhibits preference for Collagen I. Consistent with the increase in active LOX and processed LOXL2, a significant increase in Collagen I abundance and a decrease in Collagen IV abundance was noted in the aortic ECM with Ang II infusion. With the increased Collagen I accumulation, incremental elastic modulus was elevated at a high strain of 2.5. This is conventionally considered to be a region governed by collagen deformation **(Figure 4)**. When the protein expression data from the two sexes were combined, a marked increase in full length and processed LOXL2 as well as active LOX in the aortic ECM was noted in Ang II treated WT and *Loxl2*$^{+/-}$ mice. However, *Loxl2*$^{+/-}$ mice had lower LOXL2 levels than WT mice. Thus, a single allele of LOXL2 is sufficient to activate LOXL2 protein in the aortic ECM in hypertension. This indicates a compensatory mechanism to activate matrix crosslinking in order to maintain matrix integrity as the aorta faces increasing pressure. The specific pathways and mechanisms underlying this remain to be elucidated.

Our *in vitro* experiments with HASMCs and HAECs indicate that VSMCs are a more significant source of LOXL2 under cyclic strain as is imposed by the cardiac cycle,

but ECs are not. While pathologic strain of 20% does not lead to a further increase in LOXL2 abundance, it did result in higher levels of processed LOXL2. When taken together with the results from the aorta, these findings suggest that VSMCs (and not ECs) are the primary source of increased LOXL2 abundance in the aortic ECM in Ang II-induced hypertension, and the increase in LOXL2 not the result of mechanosensing. Prior studies show that loss of NO bioavailability can result in LOXL2 activation in the vascular ECM – thus, the effect of other factors such as inflammation and downstream effects of Ang II signal transduction on LOXL2 regulation could be responsible for LOXL2 activation in hypertension, and these remain to be tested in the future. Additionally, whether or not adventitial fibroblasts are another source of LOXL2 in the vasculature and whether these respond to biomechanical strain also remains to be tested. Interestingly, LOXL2's catalytic function was found to be important with regard to VSMC orientation in response to cyclic loading. This may be due to LOXL2's ability to deposit Collagen IV, which is known to promote cell orientation/ polarity. This may in part explain the critical role of LOXL2 in vasculogenesis, and remains to be further studied.

In conclusion, when considering the timeline of hypertension development, in vivo stiffness, passive aortic mechanics, and vascular reactivity results together, significant differences emerged between the sexes. In males, LOXL2 depletion delayed the onset of hypertension, prevented in vivo aortic stiffening, and prevented weight loss with Ang II infusion. LOXL2 depletion also led to improved passive mechanical properties and reduced aortic remodeling and preserved vascular reactivity. Thus, in males, LOXL2 appears to act through ECM remodeling and impaired VSMC function to contribute to aortic stiffening in hypertension. In females, while ECM remodeling was not apparent with respect to incremental modulus/mechanical testing in hypertensive WT or *Loxl2*$^{+/-}$ mice, the differences in vascular reactivity were remarkable. Specifically, LOXL2 depletion enhanced phenylephrine induced contractility, and LOXL2 depletion was consistent with reduced endothelial function. LOXL2 depletion was also associated with worsening cardiac hypertrophy in females with hypertension. Thus, in conclusion while targeting LOXL2 provided clear benefits in male hypertensives, the results in females are not favorable. Therefore, we conclude that LOXL2 is promising target to improve aortic stiffness and vascular function in hypertensive males, but not females.

Sources of Funding

The work was supported by an NHLBI grant R01HL148112 (L.S.), a Stimulating and Advancing ACCM Research (StAAR) grant from the Department of Anesthesiology and Critical Care Medicine, Johns Hopkins University (L.S.), an AHA pre-doctoral fellowship award 20PRE35120060 (H.W.), an R01HL146436 grant (D.K.), and an R01HL164936 grant (D.K.)

Disclosures

None

Figure Legends:

Figure 1. Angiotensin II (Ang II) infusion induced hypertension in males and females. (A) Schematic showing experimental timeline and endpoints. **(B)** Time course of systolic blood pressure (BP) of male (M) WT and *Loxl2*$^{+/-}$ mice with and without Ang II infusion (n = 8 for WT control, n = 8 for WT + Ang II, n = 8 for *Loxl2*$^{+/-}$ control, and n = 7 for *Loxl2*$^{+/-}$ +Ang II. At 1 wk: $^{**}p < 0.01$ for WT Ang II M vs. WT control M; at 2 wks: $^{***}p < 0.001$ for WT Ang II M vs. WT control M, $^{**}p < 0.01$ for *Loxl2*$^{+/-}$ Ang II M vs. *Loxl2*$^{+/-}$ control M; at 3 wks: $^{*}p < 0.05$ for WT Ang II M vs. WT control M, $^{****}p < 0.0001$ for *Loxl2*$^{+/-}$ Ang II M vs. *Loxl2*$^{+/-}$ control M, by repeated measures 2-way ANOVA with Bonferroni *post hoc* analysis). **(C)** Time course of systolic BP of female (F) WT and *Loxl2*$^{+/-}$ mice with and without Ang II infusion (n = 10 WT control, n = 8 WT+Ang II, n=8 *Loxl2*$^{+/-}$ control, n = 8 and *Loxl2*$^{+/-}$ +Ang II. At 1 wk: $^{*}p < 0.05$ for WT Ang II F vs. WT control F; at 2 wks: $^{*}p < 0.05$ for WT Ang II F vs. WT control F, $^{*}p < 0.05$ for *Loxl2*$^{+/-}$ Ang II F vs. *Loxl2*$^{+/-}$ control F; at 3 wks: $^{**}p < 0.01$ for WT Ang II F vs. WT control F, by repeated measures 2-way ANOVA with Bonferroni *post hoc* analysis. **(Di)** body weight of male WT and *Loxl2*$^{+/-}$ mice at the end of the experimental period (n= 12 for WT controls, n = 6 for WT+Ang II, n = 8 for *Loxl2*$^{+/-}$ controls and n = 7 for *Loxl2*$^{+/-}$ + Ang II; * p< 0.01, ****p<0.0001 by 2-way ANOVA with Bonferroni *post hoc* analysis). **(Dii)** heart weight/ body weight ratios as an index of cardiac hypertrophy at the end of 3 weeks (n= 12 for WT controls, n = 6 for WT+Ang II, n = 8 for *Loxl2*$^{+/-}$ controls and n = 7 for *Loxl2*$^{+/-}$ + Ang II; * p< 0.05, ****p<0.0001 by 2-way ANOVA with Bonferroni *post hoc* analysis). **(Ei)** body weight of female WT and *Loxl2*$^{+/-}$ mice at the end of the experimental period (n= 10 for WT controls, n = 7 for WT+Ang II, n = 11 for *Loxl2*$^{+/-}$ controls and n = 7 for*Loxl2*$^{+/-}$ + Ang II). **(Eii)** heart weight/ body weight ratios as an index of cardiac hypertrophy at the end of 3 weeks (n= 10 for WT controls, n = 7 for WT+Ang II, n = 11 for *Loxl2*$^{+/-}$ controls and n = 7 for *Loxl2*$^{+/-}$ + Ang II; ** p< 0.01 by 2-way ANOVA with Bonferroni *post hoc* analysis).

Figure 2. In vivo arterial stiffness assessment with Ang II induced hypertension in WT and *Loxl2*$^{+/-}$ male and female mice. (A) Pulse wave velocity (PWV) in male WT and *Loxl2*$^{+/-}$ mice with and without Ang II infusion (n = 8 for WT control, n = 8 for WT+Ang II, n=8 for *Loxl2*$^{+/-}$ control, and n = 7 for *Loxl2*$^{+/-}$ +Ang II. At 3 wks: $^{**}p < 0.01$ for WT Ang II M vs. WT control M, by repeated measures 2-way ANOVA with Bonferroni *post hoc* analysis; **(B)** PWV in female WT and *Loxl2*$^{+/-}$ mice with and without Ang II infusion (n = 10 WT control, n = 8 WT+Ang II, n=8 *Loxl2*$^{+/-}$ control, n = 8 and *Loxl2*$^{+/-}$ +Ang II).

Figure 3. Vasoreactivity of aortae from WT and *Loxl2*$^{+/-}$ mice. Analysis of aortic rings from **(A)** male and **(B)** female mice to increasing concentrations of phenylephrine (PE; **Ai:** male, **Bi:** female), calculated as percentage of max KCL-induced vasoconstriction, Acetylcholine (Ach) - induced endothelium-dependent vasorelaxation of vessels pre-constricted by PE (**Aii:** male, **Bii:** female), and Endothelium-independent vasorelaxation in response of PE pre-constricted rings to increasing concentrations of sodium nitroprusside (SNP) (**Aiii:** male, **Biii:** female) (n = 7 – 10 mice per cohort; two rings were assessed from each animal. $^{*}p < 0.05$, $^{**}p < 0.01$, $^{***}p < 0.001$ by repeated measures 2-Way ANOVA).

Figure 4. Effects of Ang II infusion on passive mechanical properties of the aorta in male and female WT and *Loxl2*$^{+/-}$ mice. Uniaxial tensile testing of intact and decellularized aortic segments from male and female WT and *Loxl2*$^{+/-}$ mice with and without Ang II infusion. **(A)** Stress-strain curves of intact aortic rings from male **(Ai)**WT**,** **(Aii)** male *Loxl2*$^{+/-}$ mice. Data are shown as mean (solid line)□±□standard error (dotted lines). Incremental elastic modulus of intact aortic segments at **(Aiii)** low strain (0.5) in and **(Aiv)** high strain (2.5). **(B)** Stress-strain relationships of decellularized aortic rings from **(Bi)**male WT and **(Bii)**male *Loxl2*$^{+/-}$ mice. Incremental elastic modulus of decellularized aortic segments at **(Biii)** low strain (0.5) in and **(Biv)** high strain (2.5). **(C)** Ultimate stress at failure of **(Ci)** intact and **(Cii)** decellularized aortic rings from males. **(D)** Strain at failure of **(Di)** intact and **(Dii)** decellularized aortic rings from male mice.

(E) Stress-strain curves of intact aortic rings from **(Ei)**female WT**,** **(Eii)** male *Loxl2*$^{+/-}$ mice. Data are shown as mean (solid line)□±□standard error (dotted lines). Incremental elastic modulus of intact aortic segments at **(Eiii)** low strain (0.5) in and **(Eiv)** high strain (2.5). **(F)** Stress-strain relationships of decellularized aortic rings from **(Fi)** female WT and **(Fii)** *Loxl2*$^{+/-}$ mice. Incremental elastic modulus of decellularized aortic segments at **(Fiii)** low strain (0.5) in and **(Fiv)** high strain (2.5). **(G)** Ultimate stress at failure of **(Gi)** intact and **(Gii)** decellularized aortic rings from females. **(H)** Strain at failure of **(Hi)** intact and **(Hii)** decellularized aortic rings from male mice.

(n = 14-22 aortic rings; 2 rings were tested from n = 7-11 mice in each group; ****p<0.0001 by repeated measures 2-way ANOVA with Bonferroni post-hoc analysis for stress vs strain curves; **p<0.01, ***p<0.001 by 2- way ANOVA with Bonferroni post-hoc analysis for scatter plots).

Figure 5. Histochemical analysis of aorta from WT and *Loxl2*$^{+/-}$ mice. (A) Representative Hematoxylin and Eosin, Masson's Trichrome and Movat pentachrome stains in **(Ai)** male and **(Aii)** female mice. (**B)** VSMC nuclei in vascular wall (**Bi:** males, **Bii:** females), **(C)** Lumen diameter (**Ci:** males, **Cii:** females), and **(D)** wall thickness (**Di:** males, **Dii:** females), and **(E)** intralamellar distance (**Ei:** males, **Eii:** females) of the aorta rings were calculated from H&E stained images. (n = 5-7 for each group, **p < 0.01, and ****p < 0.0001 by 2-way ANOVA).

Figure 6. Assessment of protein expression in aortic ECM. Western blotting of aortic ECM from *Loxl2*$^{+/-}$ and littermate WT mice with and without Ang II infusion. Representative Western blots showing expression of LOXL2, LOX and COL I in the extracellular matrix (ECM), fraction of aorta extracted 3 wks after initiation of experiment (**Ai:** males, **Bi:** females). Densitometry analyses of full length LOXL2 **(Aii:** males, **Bii:** females**)**, processed C-terminus fragment of LOXL2 **(Aiii:** males, **Biii:** females**)**, pro-LOX **(Aiv:** males, **Biv:** females**)**, processed, active LOX (**Av:** males, **Bv:** females), Collagen I (**Avi:** males, **Bvi:** females), and Collagen IV (**Avii:** males, **Bvii:** females). (n = 5-9 mice per group; *p < 0.05, **p < 0.01, and ***p < 0.001 by 2-way ANOVA).

Figure 7. LOXL2 abundance increased with cyclic strain in VSMCs but not ECs. (A) representative phase contrast images of HASMC **(Ai)** and HAECs **(Aii)** under static, 10% or 20% cyclic strain. Scale bar = 50 µm. Double-headed arrow indicates the strain vector. **(B, C)** Representative Western blots and densitometry analysis of LOXL2 expression in **(B)** human aortic smooth muscle cell (HASMC; n = 13 per group and **(C)**

human aortic endothelial cell (HAEC; n = 4 per group) (*$p < 0.05$, **$p < 0.01$ by ordinary 1-way ANOVA with Bonferroni post hoc analysis.).

Figure 8. LOXL2 plays an important role in VSMC alignment. Wild-type (WT) HASMCs ± PAT-1251 (10μM) and LOXL2 knocked-out (T1) HASMCs ± Ad-LOXL2-enriched media were static or stretched at 20% on FN-coated PDMS chambers. **(A)** Representative confocal microscopy images of formalin-fixed cells stained with FITC-phalloidin (green). Scale bar = 400 μm. Stretched cells aligned perpendicular to direction of stretch. Representative cumulative compass plots show the proportions of actin fibers at each angle. **(B)** Representative Western blotting of cell culture media post 24-hr stretch. LOXL2 was immunodetected. **(C)** CurveAlign was used to identify actin fibers and assign vectors to all actin fibers stained with phalloidin. The intensity of fibers in the same angle is characterized by alignment coefficient. (Number of x5 magnification confocal images n = 3-4 per group, with 500+ cells per image, **$p < 0.01$, ****$p < 0.0001$ by 2-way ANOVA).

Supplemental Figures:

Supplemental Figure S1. Systolic BP, Diastolic BP and mean arterial pressure (MAP) for all groups. n = 8-10 for each group.

Supplemental Figure S2. Heart rate during PWV measurement for all groups. n = 8-10 for each group.

Supplemental Figure S3: Densitometry analysis of Western blots with both sexes combined. (A) full length LOXL2, (**B)** Processed LOXL2, (**C)** Pro-LOX, (**D)** active LOX, (**E)** Collagen I, and (**F)** Collagen IV expression in the aortic ECM.

References:

1. Brown DW, Giles WH, Greenlund KJ. Blood pressure parameters and risk of fatal stroke, NHANES II mortality study. *Am J Hypertens*. 2007;20:338-341. doi: 10.1016/j.amjhyper.2006.08.004
2. Lewington S, Clarke R, Qizilbash N, Peto R, Collins R, Prospective Studies C. Age-specific relevance of usual blood pressure to vascular mortality: a meta-analysis of individual data for one million adults in 61 prospective studies. *Lancet*. 2002;360:1903-1913. doi: 10.1016/s0140-6736(02)11911-8
3. Frohlich ED. Cardiac hypertrophy in hypertension. *N Engl J Med*. 1987;317:831-833. doi: 10.1056/NEJM198709243171310
4. Healey JS, Connolly SJ. Atrial fibrillation: hypertension as a causative agent, risk factor for complications, and potential therapeutic target. *Am J Cardiol*. 2003;91:9G-14G. doi: 10.1016/s0002-9149(03)00227-3
5. Levy D, Larson MG, Vasan RS, Kannel WB, Ho KK. The progression from hypertension to congestive heart failure. *JAMA*. 1996;275:1557-1562.
6. McInnes GT. Hypertension and coronary artery disease: cause and effect. *J Hypertens Suppl*. 1995;13:S49-56. doi: 10.1097/00004872-199508001-00008
7. Mills KT, Stefanescu A, He J. The global epidemiology of hypertension. *Nat Rev Nephrol*. 2020;16:223-237. doi: 10.1038/s41581-019-0244-2
8. Egan BM, Li J, Sutherland SE, Rakotz M, Wozniak G. Abstract MP33: Hypertension Control In The Us 2009 To 2018: Rapidly Reversing Years Of Progress. *Hypertension*. 2020;76:AMP33-AMP33.
9. Mitchell GF, Guo CY, Benjamin EJ, Larson MG, Keyes MJ, Vita JA, Vasan RS, Levy D. Cross-sectional correlates of increased aortic stiffness in the community: the Framingham Heart Study. *Circulation*. 2007;115:2628-2636. doi: 10.1161/CIRCULATIONAHA.106.667733
10. Mitchell GF. Arterial stiffness and hypertension: chicken or egg? *Hypertension*. 2014;64:210-214. doi: 10.1161/HYPERTENSIONAHA.114.03449
11. Steppan J, Wang H, Bergman Y, Rauer MJ, Tan S, Jandu S, Nandakumar K, Barreto-Ortiz S, Cole RN, Boronina TN, et al. Lysyl oxidase-like 2 depletion is protective in age-associated vascular stiffening. *Am J Physiol Heart Circ Physiol*. 2019;317:H49-H59. doi: 10.1152/ajpheart.00670.2018
12. Wang H, Poe A, Pak L, Nandakumar K, Jandu S, Steppan J, Loser R, Santhanam L. An in situ activity assay for lysyl oxidases. *Commun Biol*. 2021;4:840. doi: 10.1038/s42003-021-02354-0
13. Yang J, Savvatis K, Kang JS, Fan P, Zhong H, Schwartz K, Barry V, Mikels-Vigdal A, Karpinski S, Kornyeyev D, et al. Targeting LOXL2 for cardiac interstitial fibrosis and heart failure treatment. *Nat Commun*. 2016;7:13710. doi: 10.1038/ncomms13710
14. Wu Y, Can J, Hao S, Qiang X, Ning Z. LOXL2 Inhibitor Attenuates Angiotensin II-Induced Atrial Fibrosis and Vulnerability to Atrial Fibrillation through Inhibition of Transforming Growth Factor Beta-1 Smad2/3 Pathway. *Cerebrovasc Dis*. 2021:1-11. doi: 10.1159/000518526
15. Zhao Y, Tang K, Tianbao X, Wang J, Yang J, Li D. Increased serum lysyl oxidase-like 2 levels correlate with the degree of left atrial fibrosis in patients with atrial fibrillation. *Biosci Rep*. 2017;37. doi: 10.1042/BSR20171332

16. Wu Y, Li Z, Shi Y, Chen L, Tan H, Wang Z, Yin C, Liu L, Hu J. Exome Sequencing Identifies LOXL2 Mutation as a Cause of Familial Intracranial Aneurysm. *World Neurosurg*. 2018;109:e812-e818. doi: 10.1016/j.wneu.2017.10.094
17. Poe A, Martinez Yus M, Wang H, Santhanam L. Lysyl oxidase like-2 in fibrosis and cardiovascular disease. *Am J Physiol Cell Physiol*. 2023;325:C694-C707. doi: 10.1152/ajpcell.00176.2023
18. Hartley CJ, Taffet GE, Michael LH, Pham TT, Entman ML. Noninvasive determination of pulse-wave velocity in mice. *Am J Physiol*. 1997;273:H494-500. doi: 10.1152/ajpheart.1997.273.1.H494
19. Barreto Ortiz S, Hori D, Nomura Y, Yun X, Jiang H, Yong H, Chen J, Paek S, Pandey D, Sikka G, et al. Opsin 3 and 4 mediate light-induced pulmonary vasorelaxation that is potentiated by G protein-coupled receptor kinase 2 inhibition. *Am J Physiol Lung Cell Mol Physiol*. 2018;314:L93-L106. doi: 10.1152/ajplung.00091.2017
20. Jung SM, Jandu S, Steppan J, Belkin A, An SS, Pak A, Choi EY, Nyhan D, Butlin M, Viegas K, et al. Increased tissue transglutaminase activity contributes to central vascular stiffness in eNOS knockout mice. *Am J Physiol Heart Circ Physiol*. 2013;305:H803-810. doi: 10.1152/ajpheart.00103.2013
21. Steppan J, Sikka G, Jandu S, Barodka V, Halushka MK, Flavahan NA, Belkin AM, Nyhan D, Butlin M, Avolio A, et al. Exercise, vascular stiffness, and tissue transglutaminase. *Journal of the American Heart Association*. 2014;3:e000599. doi: 10.1161/JAHA.113.000599
22. Steppan J, Bergman Y, Viegas K, Armstrong D, Tan S, Wang H, Melucci S, Hori D, Park SY, Barreto SF, et al. Tissue Transglutaminase Modulates Vascular Stiffness and Function Through Crosslinking-Dependent and Crosslinking-Independent Functions. *Journal of the American Heart Association*. 2017;6. doi: 10.1161/JAHA.116.004161
23. Wang H, Chen J, Jandu S, Melucci S, Savage W, Nandakumar K, Kang SK, Barreto-Ortiz S, Poe A, Rastogi S, et al. Probing tissue transglutaminase mediated vascular smooth muscle cell aging using a novel transamidation-deficient Tgm2-C277S mouse model. *Cell Death Discov*. 2021;7:197. doi: 10.1038/s41420-021-00543-8
24. Wang H, Poe A, Martinez Yus M, Pak L, Nandakumar K, Santhanam L. Lysyl oxidase-like 2 processing by factor Xa modulates its activity and substrate preference. *Commun Biol*. 2023;6:375. doi: 10.1038/s42003-023-04748-8
25. Takane K, Hasegawa Y, Lin B, Koibuchi N, Cao C, Yokoo T, Kim-Mitsuyama S. Detrimental Effects of Centrally Administered Angiotensin II are Enhanced in a Mouse Model of Alzheimer Disease Independently of Blood Pressure. *Journal of the American Heart Association*. 2017;6. doi: 10.1161/JAHA.116.004897
26. Foulquier S, Namsolleck P, Van Hagen BT, Milanova I, Post MJ, Blankesteijn WM, Rutten BP, Prickaerts J, Van Oostenbrugge RJ, Unger T. Hypertension-induced cognitive impairment: insights from prolonged angiotensin II infusion in mice. *Hypertens Res*. 2018;41:817-827. doi: 10.1038/s41440-018-0090-9

27. Cassis LA, Marshall DE, Fettinger MJ, Rosenbluth B, Lodder RA. Mechanisms contributing to angiotensin II regulation of body weight. *Am J Physiol*. 1998;274:E867-876. doi: 10.1152/ajpendo.1998.274.5.E867
28. Grimsby JL, Lucero HA, Trackman PC, Ravid K, Kagan HM. Role of lysyl oxidase propeptide in secretion and enzyme activity. *J Cell Biochem*. 2010;111:1231-1243. doi: 10.1002/jcb.22845
29. Anwar MA, Shalhoub J, Lim CS, Gohel MS, Davies AH. The effect of pressure-induced mechanical stretch on vascular wall differential gene expression. *J Vasc Res*. 2012;49:463-478. doi: 10.1159/000339151
30. Jufri NF, Mohamedali A, Avolio A, Baker MS. Mechanical stretch: physiological and pathological implications for human vascular endothelial cells. *Vasc Cell*. 2015;7:8. doi: 10.1186/s13221-015-0033-z

Figure 1

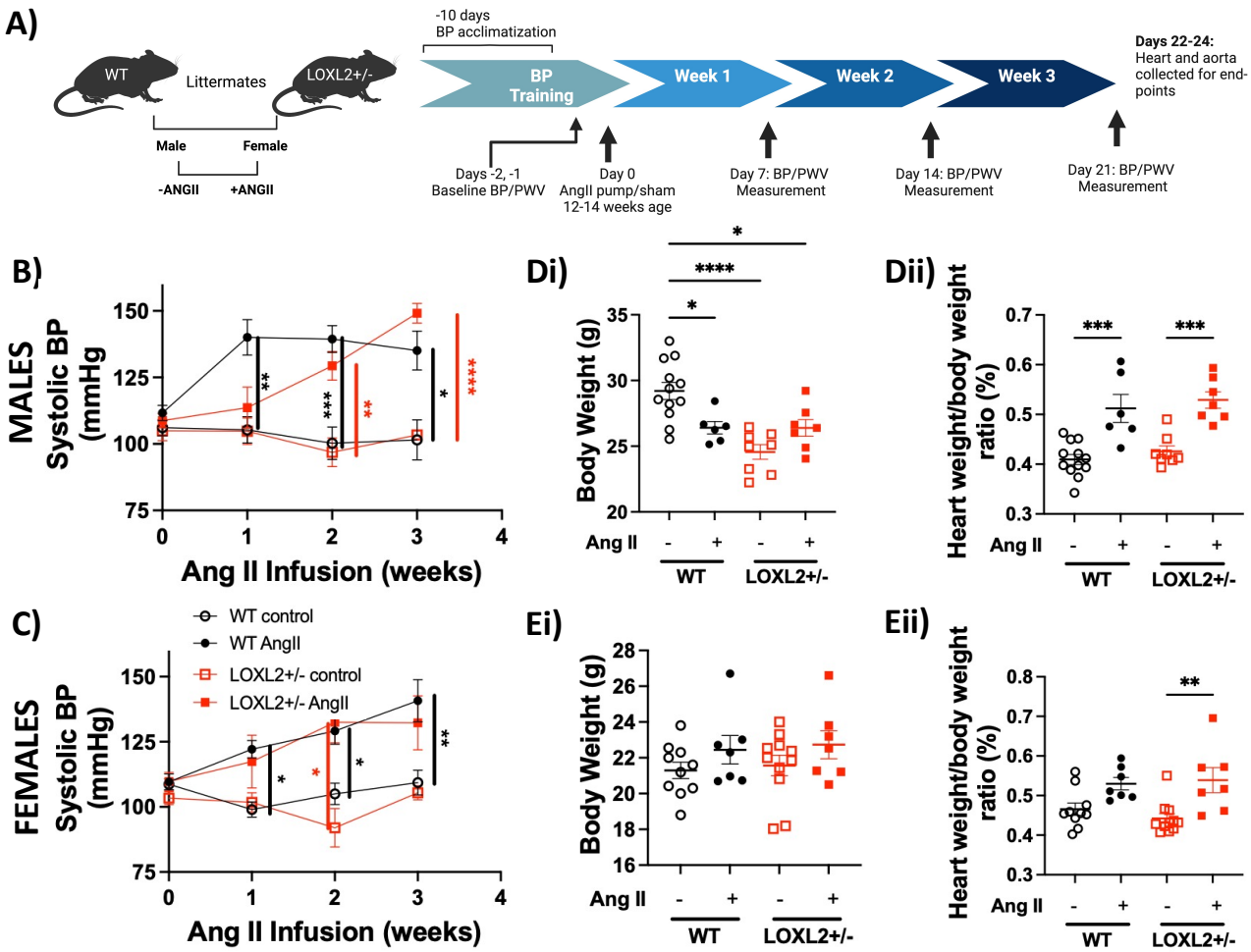
A)
WT
Littermates
LOXL2+/-
Male
Female
-ANGII
+ANGII
-10 days
BP acclimatization
BP Training
Week 1
Week 2
Week 3
Days 22-24:
Heart and aorta collected for end-points
Days -2, -1
Baseline BP/PWV
Day 0
AngII pump/sham
12-14 weeks age
Day 7: BP/PWV Measurement
Day 14: BP/PWV Measurement
Day 21: BP/PWV Measurement
B)
MALES
Systolic BP (mmHg)
Ang II Infusion (weeks)
Di)
Body Weight (g)
Ang II
WT
LOXL2+/-
Dii)
Heart weight/body weight ratio (%)
C)
FEMALES
WT control
WT AngII
LOXL2+/- control
LOXL2+/- AngII
Ei)
Eii)

Figure 2

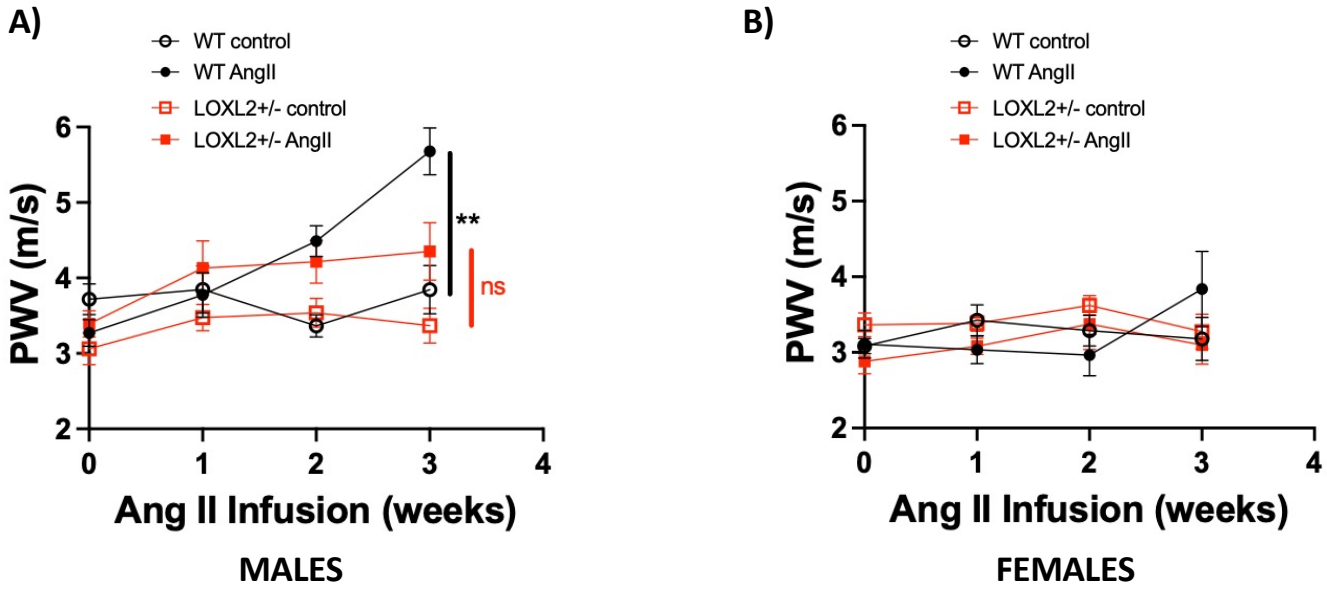
A)
WT control
WT AngII
LOXL2+/- control
LOXL2+/- AngII
PWV (m/s)
6
5
4
3
2
0
1
2
3
4
**
ns
Ang II Infusion (weeks)
MALES
B)
WT control
WT AngII
LOXL2+/- control
LOXL2+/- AngII
PWV (m/s)
6
5
4
3
2
0
1
2
3
4
Ang II Infusion (weeks)
FEMALES

Figure 3

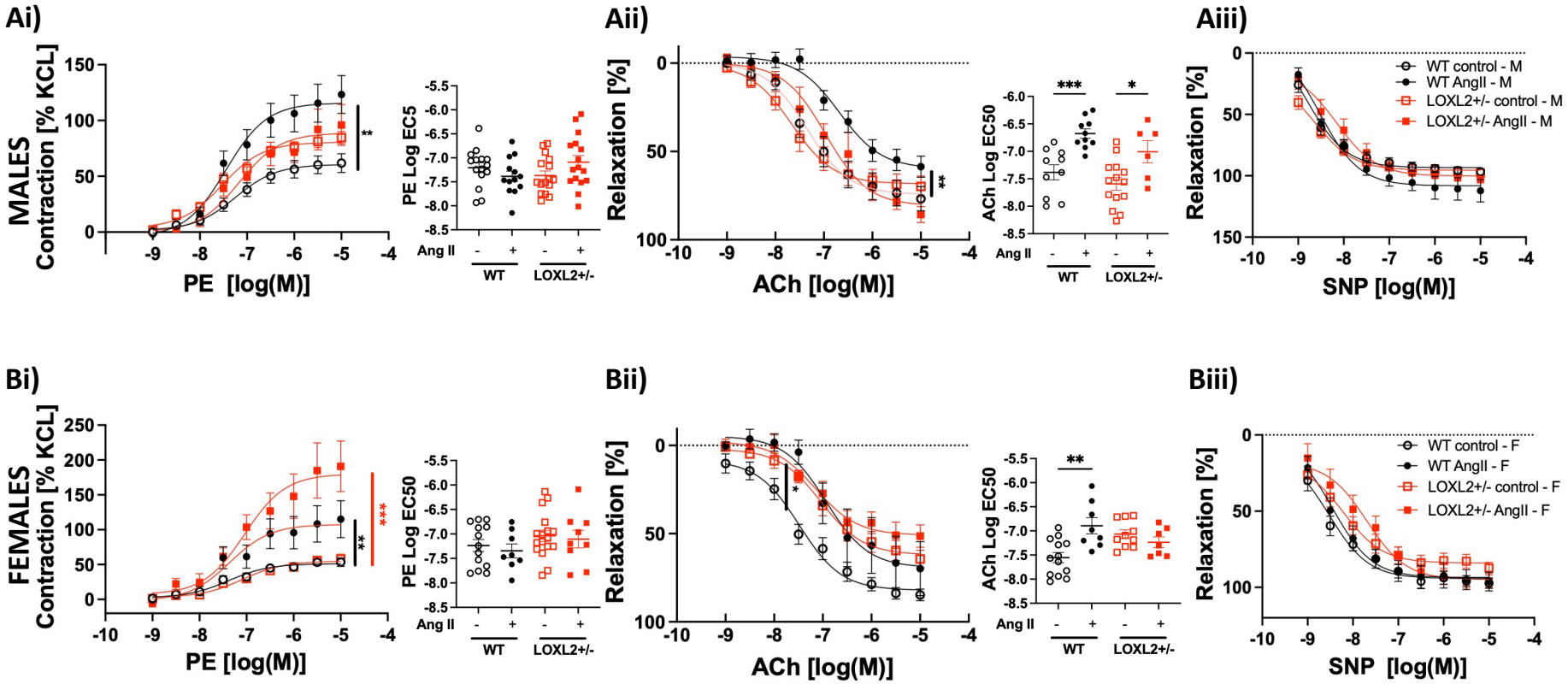
Ai)
MALES
Contraction [% KCL]
PE [log(M)]
PE Log EC5
Ang II
WT
LOXL2+/-
Aii)
Relaxation [%]
ACh [log(M)]
ACh Log EC50
Aiii)
WT control - M
WT AngII - M
LOXL2+/- control - M
LOXL2+/- AngII - M
SNP [log(M)]
Bi)
FEMALES
Contraction [% KCL]
PE [log(M)]
PE Log EC50
Bii)
ACh [log(M)]
ACh Log EC50
Biii)
WT control - F
WT AngII - F
LOXL2+/- control - F
LOXL2+/- AngII - F
SNP [log(M)]

Figure 4

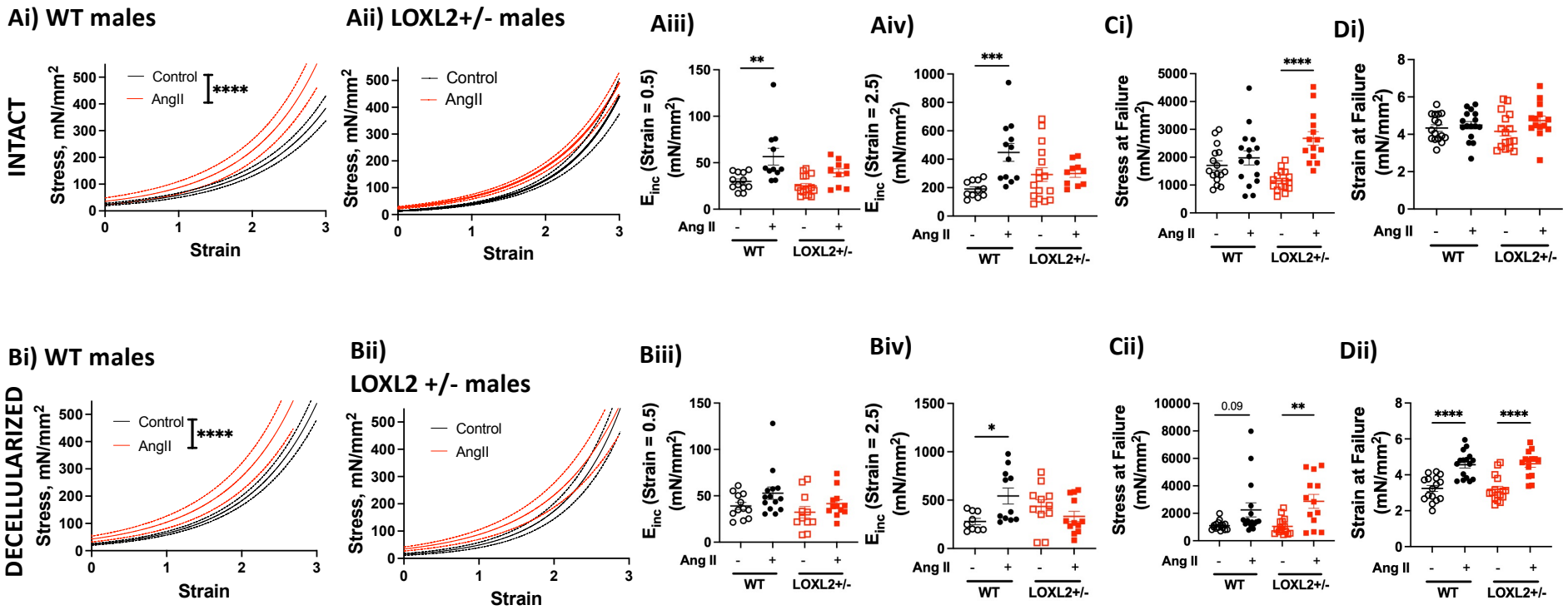
Ai) WT males
Aii) LOXL2+/- males
Aiii)
Aiv)
Ci)
Di)
INTACT
Control
AngII
****
Stress, mN/mm2
Strain
**
***
****
Einc (Strain = 0.5) (mN/mm2)
Einc (Strain = 2.5) (mN/mm2)
Stress at Failure (mN/mm2)
Strain at Failure (mN/mm2)
Ang II
WT
LOXL2+/-
Bi) WT males
Bii)
LOXL2 +/- males
Biii)
Biv)
Cii)
Dii)
DECELLULARIZED
0.09
*

Figure 4

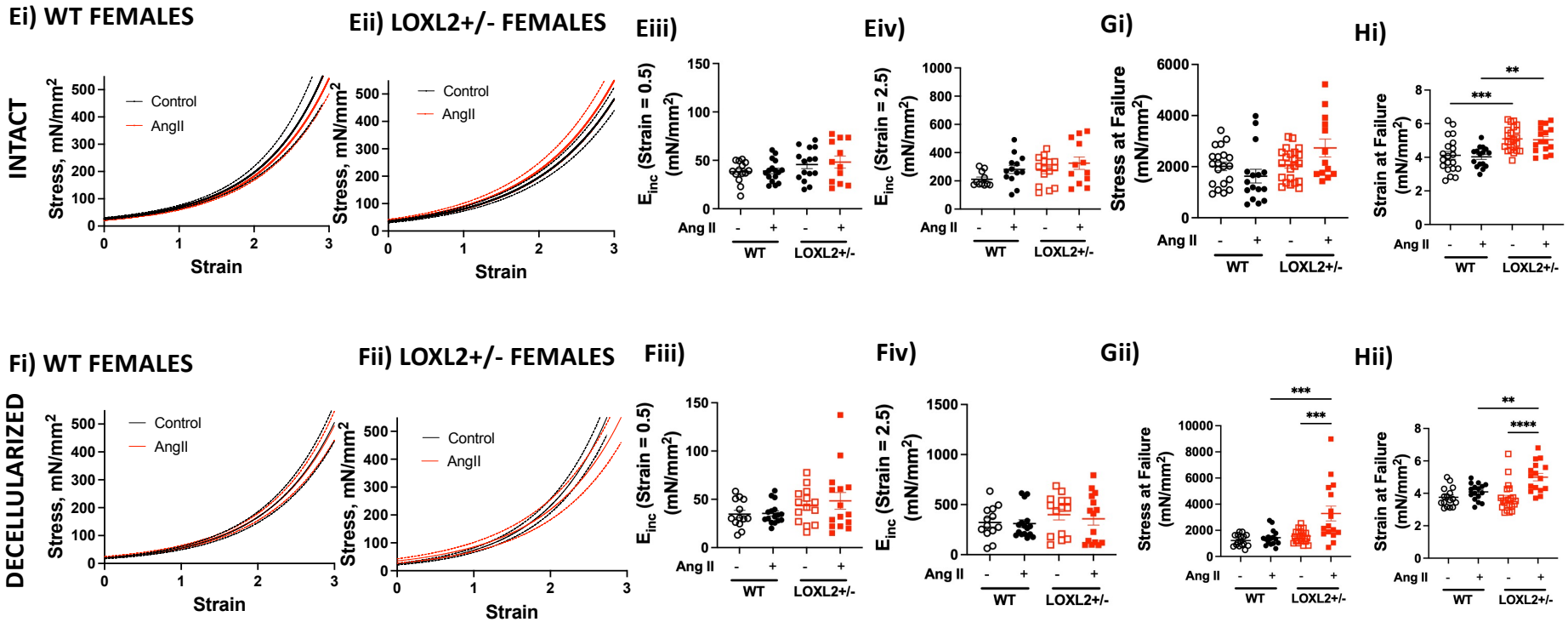
Ei) WT FEMALES
Eii) LOXL2+/- FEMALES
Eiii)
Eiv)
Gi)
Hi)
INTACT
Control
AngII
Stress, mN/mm2
Strain
Einc (Strain = 0.5) (mN/mm2)
Einc (Strain = 2.5) (mN/mm2)
Stress at Failure (mN/mm2)
Strain at Failure (mN/mm2)
Ang II
WT
LOXL2+/-
Fi) WT FEMALES
Fii) LOXL2+/- FEMALES
Fiii)
Fiv)
Gii)
Hii)
DECELLULARIZED

Figure 5

Ai) MALES

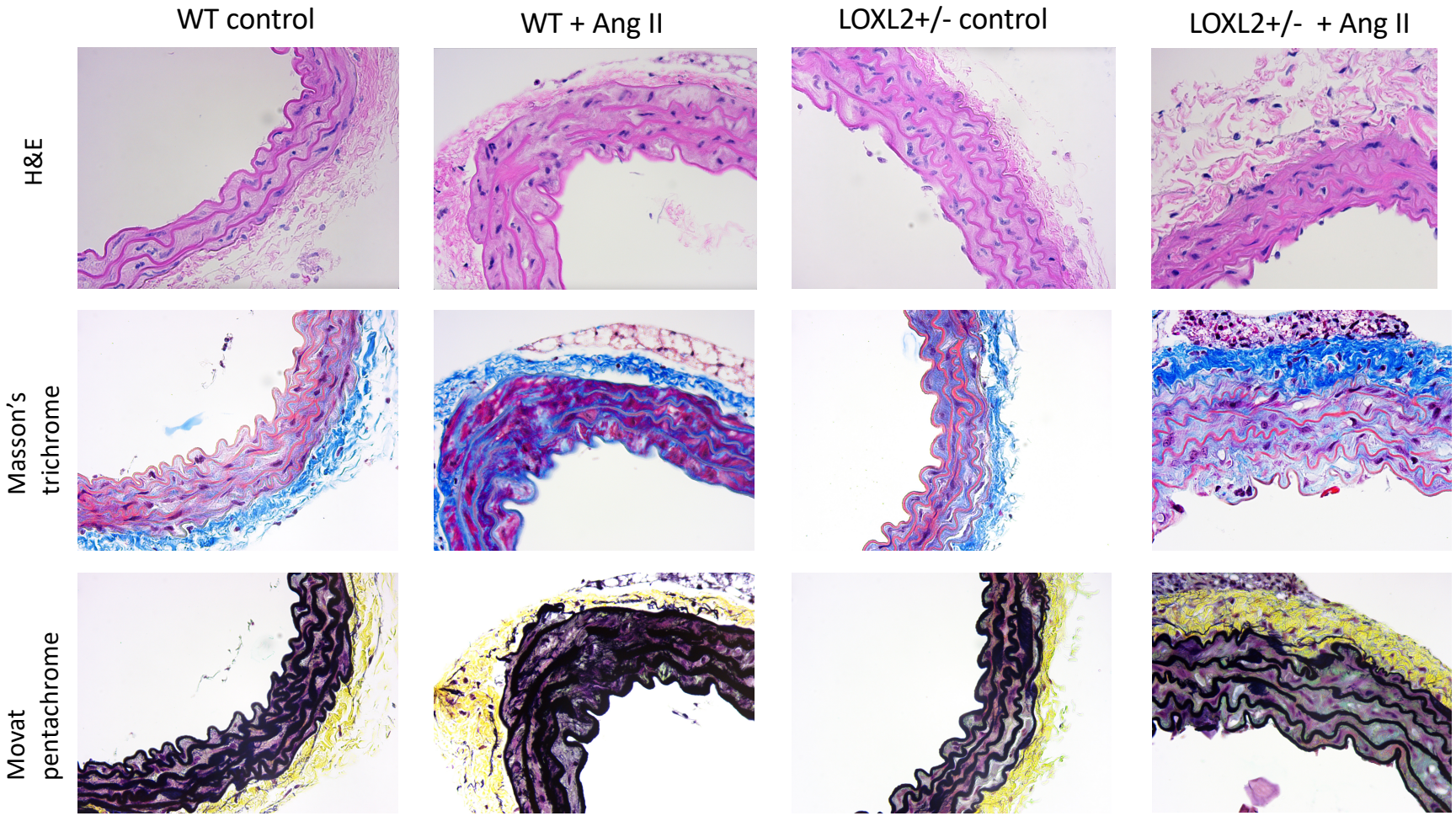

Figure 5

Aii)
FEMALES

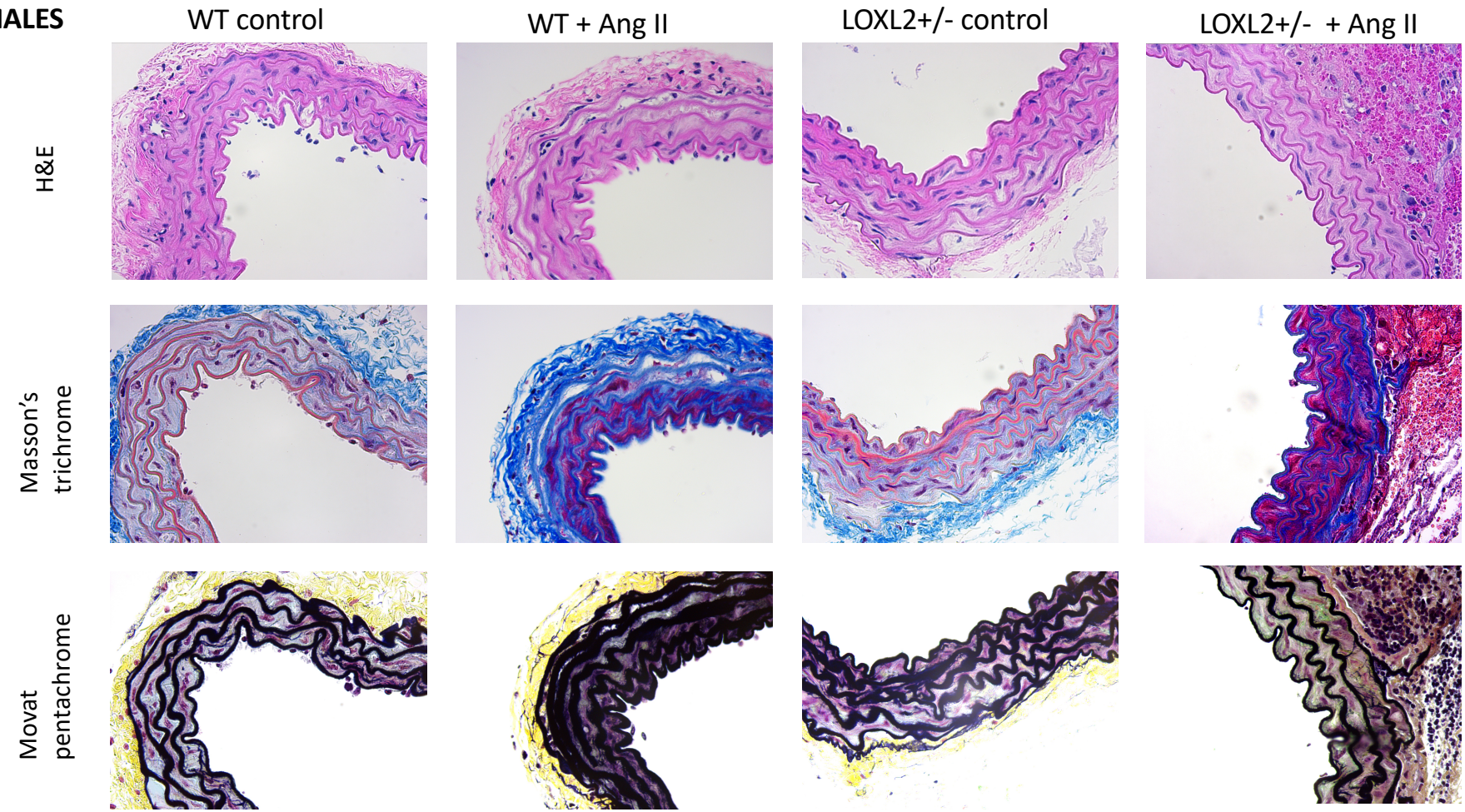

Figure 5

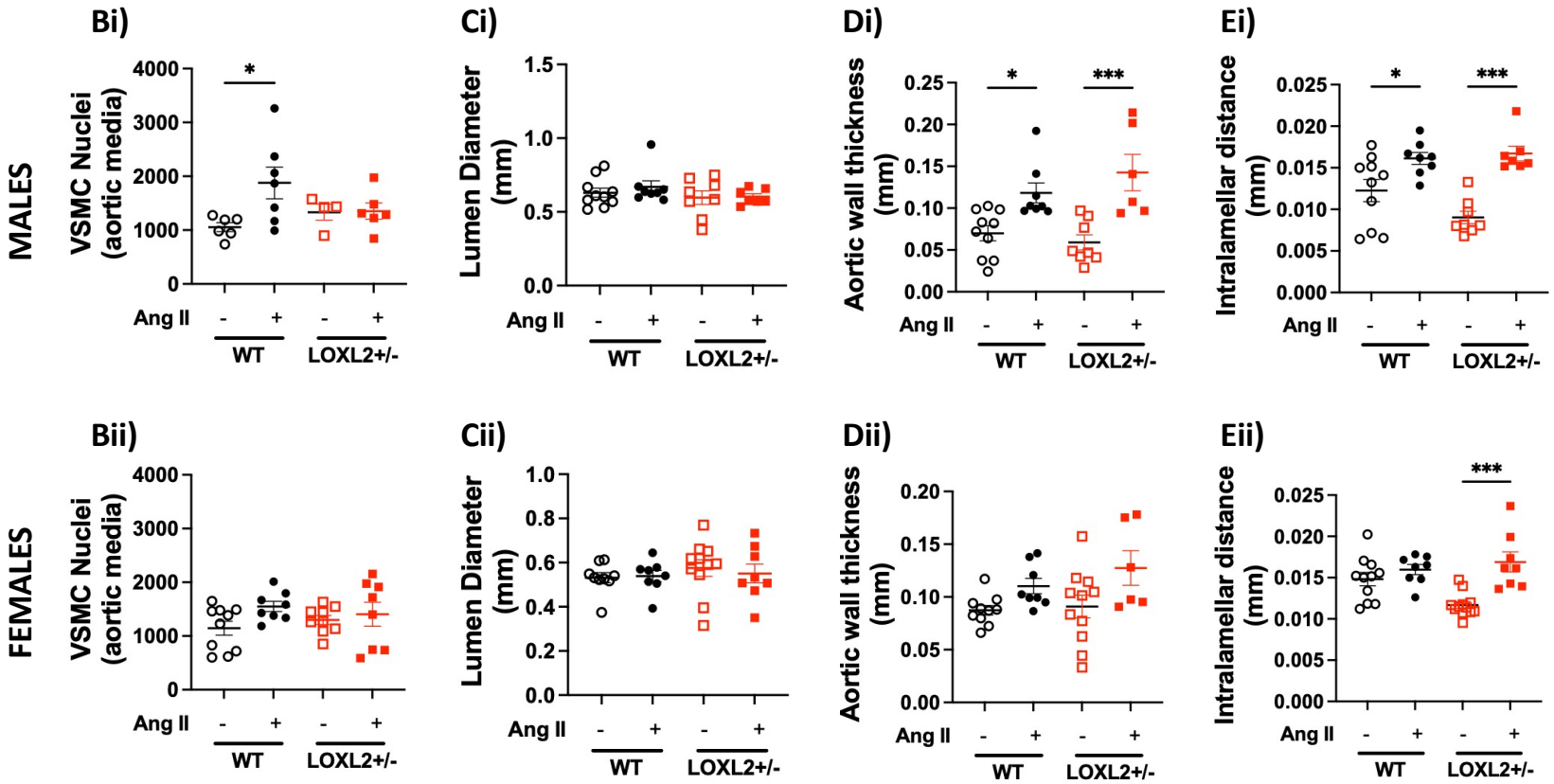
Bi)
Ci)
Di)
Ei)
MALES
VSMC Nuclei (aortic media)
Lumen Diameter (mm)
Aortic wall thickness (mm)
Intralamellar distance (mm)
Ang II
WT
LOXL2+/-
Bii)
Cii)
Dii)
Eii)
FEMALES

Figure 6

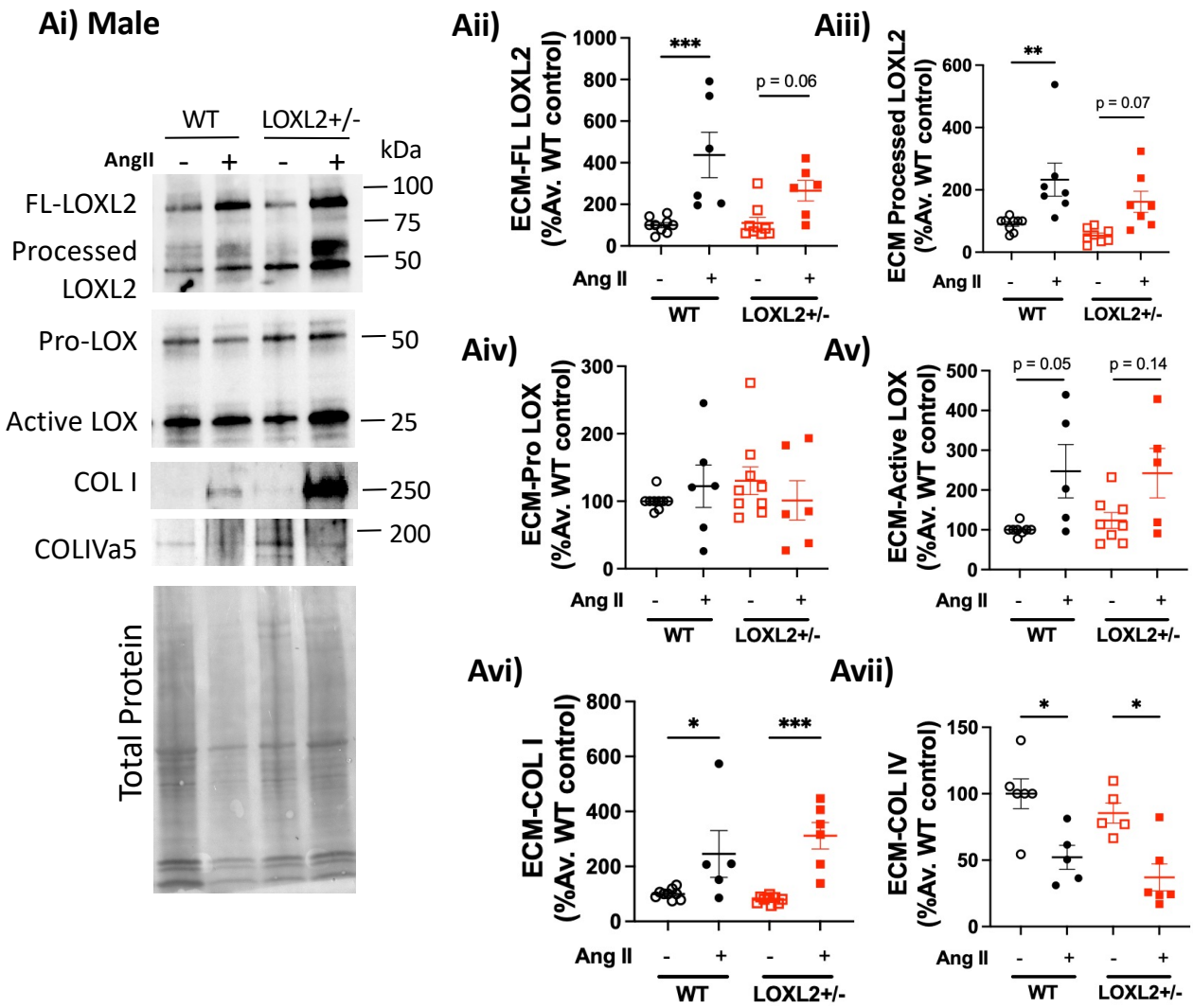
Ai) Male
WT
LOXL2+/-
AngII
kDa
FL-LOXL2
Processed LOXL2
Pro-LOX
Active LOX
COL I
COLIVa5
Total Protein
100
75
50
50
25
250
200
Aii)
ECM-FL LOXL2 (%Av. WT control)
***
p = 0.06
Aiii)
ECM Processed LOXL2 (%Av. WT control)
**
p = 0.07
Aiv)
ECM-Pro LOX (%Av. WT control)
Av)
ECM-Active LOX (%Av. WT control)
p = 0.05
p = 0.14
Avi)
ECM-COL I (%Av. WT control)
*
***
Avii)
ECM-COL IV (%Av. WT control)
*
*
Ang II
WT
LOXL2+/-

Figure 6

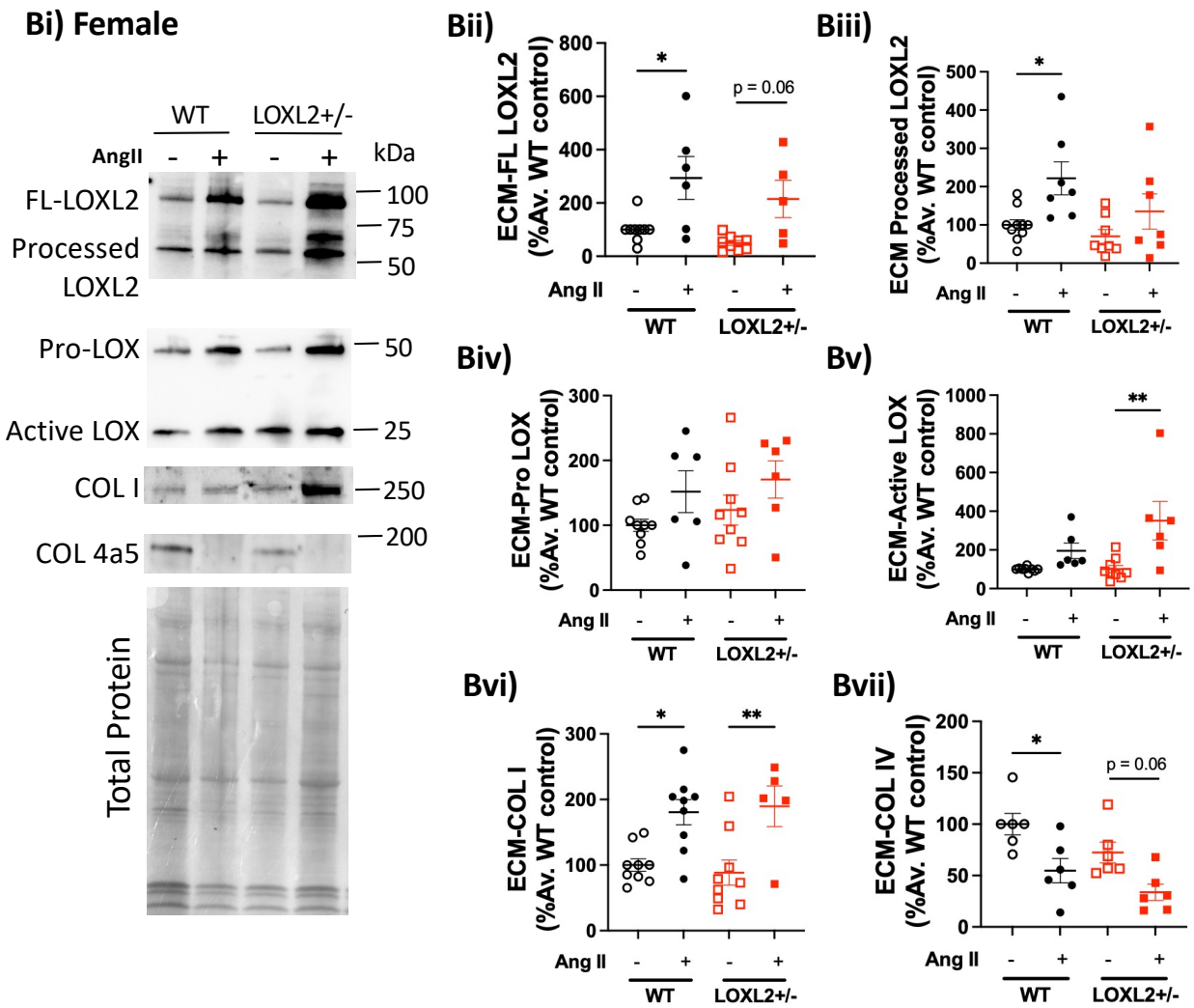
Bi) Female
WT
LOXL2+/-
AngII
- + - +
kDa
FL-LOXL2
Processed LOXL2
Pro-LOX
Active LOX
COL I
COL 4a5
Total Protein
100
75
50
50
25
250
200
Bii)
ECM-FL LOXL2 (%Av. WT control)
p = 0.06
Biii)
ECM Processed LOXL2 (%Av. WT control)
Biv)
ECM-Pro LOX (%Av. WT control)
Bv)
ECM-Active LOX (%Av. WT control)
Bvi)
ECM-COL I (%Av. WT control)
Bvii)
ECM-COL IV (%Av. WT control)
Ang II
WT
LOXL2+/-

Figure 7

Ai) HASMCs

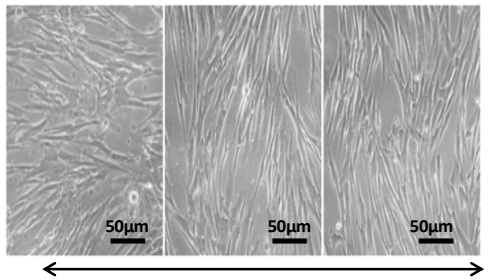

Bi)

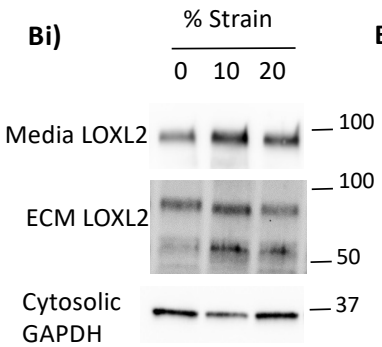

Bii)

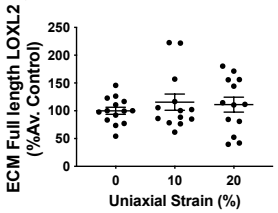

Biii)

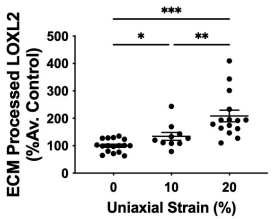

Biv)

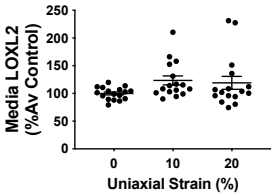

Aii) HAECs

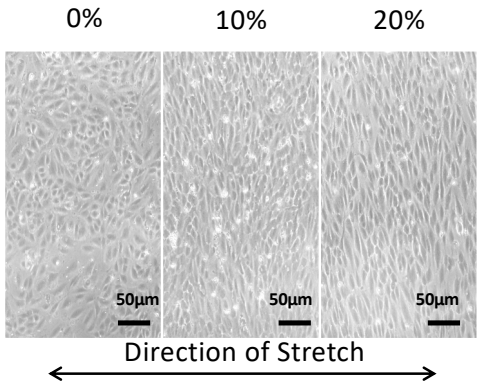

Ci)

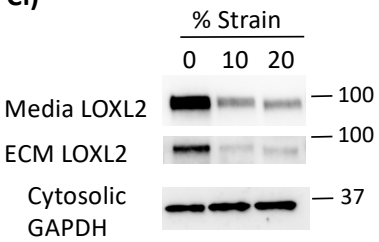

Cii)

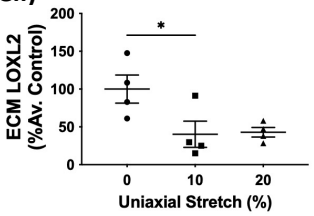

Ciii)

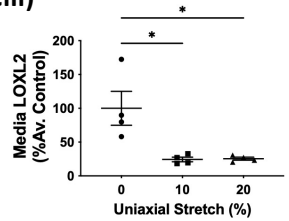

Figure 8

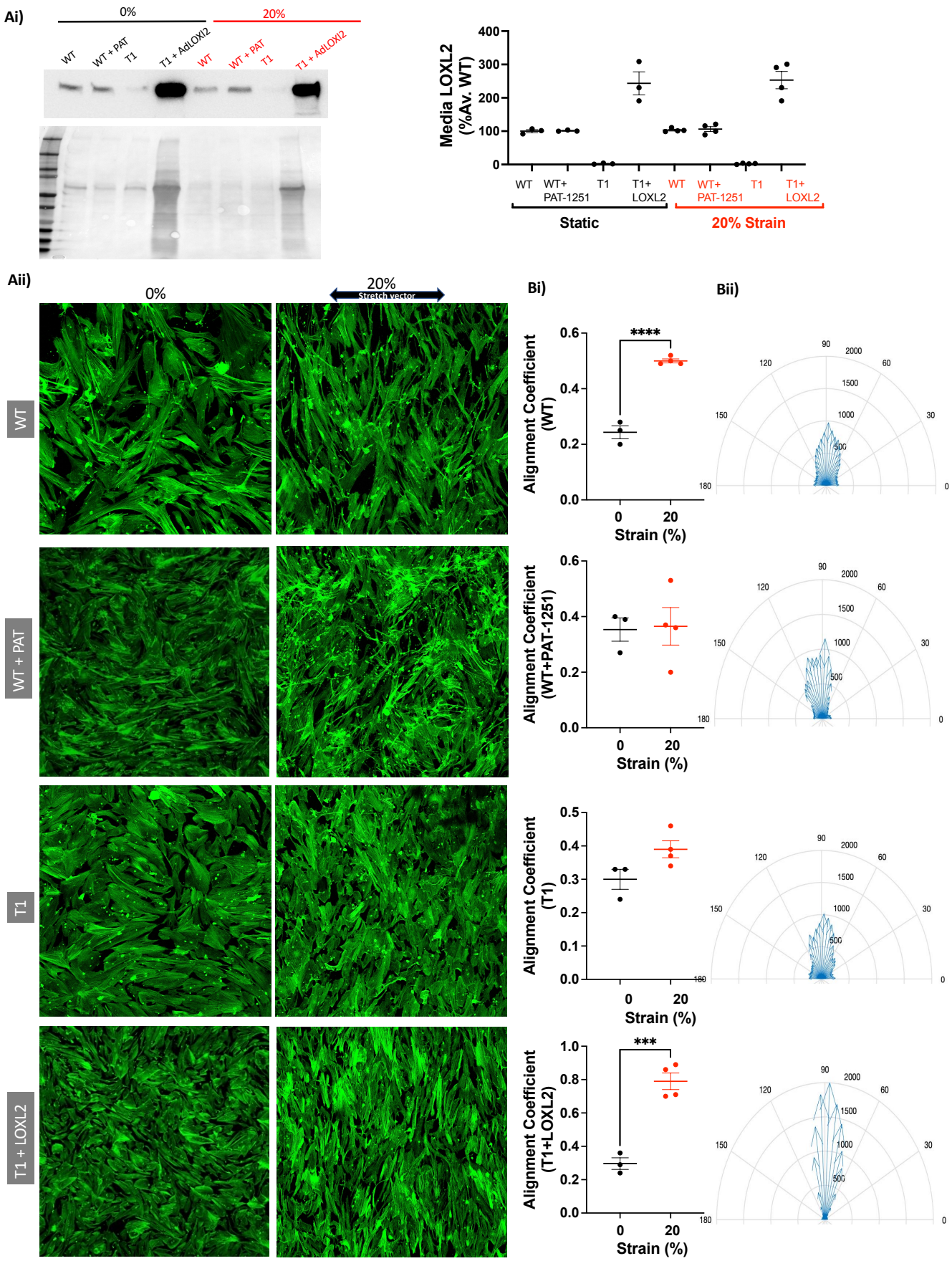
Ai)
0%
20%
WT
WT + PAT
T1
T1 + AdLOXL2
WT
WT + PAT
T1
T1 + AdLOXL2
Media LOXL2 (%Av. WT)
400
300
200
100
0
WT
WT+ PAT-1251
T1
T1+ LOXL2
WT
WT+ PAT-1251
T1
T1+ LOXL2
Static
20% Strain
Aii)
0%
20%
Stretch vector
WT
WT + PAT
T1
T1 + LOXL2
Bi)
Bii)
Alignment Coefficient (WT)
Alignment Coefficient (WT+PAT-1251)
Alignment Coefficient (T1)
Alignment Coefficient (T1+LOXL2)
****
***
Strain (%)
0
20
90
120
60
150
30
180
0
2000
1500
1000
500